

In/CdTe/Au p–n Gamma-ray Detectors Fabricated Using n-type Layer Formed by Laser-induced Back-side Doping with Nd:YAG Laser

Taku Miyake,^{1*} Junichi Nishizawa,^{1,2} Akifumi Koike,¹
Toru Aoki,^{1,2} and Hidenori Mimura^{1,2}

¹ANSeeN Inc. 3-5-1 Johoku, Naka-ku, Hamamatsu 432-8011, Japan

²Research Institute of Electronics, Shizuoka University, 3-5-1 Johoku, Naka-ku, Hamamatsu 432-8011, Japan

(Received September 21, 2023; accepted November 20, 2023)

Keywords: laser doping, pn diode, CdTe gamma-ray detector, indium doping

An n-type layer was formed in p-type CdTe via the laser-induced back-side doping of In with a Nd:YAG laser. Hall effect measurements confirmed the formation of an n-type layer on the In-doped area. The In/CdTe/Au p–n diode was fabricated as a gamma-ray detector via laser-induced back-side doping. A guard-ring structure was introduced into the In anode electrode to realize an electron-collecting-type detector with a low leakage current, although pixelation on the In anode side was difficult. In the In/CdTe/Au p–n gamma-ray detector, rectification behavior was clearly observed, and the leakage current of the central electrode was 13 nA at a reverse voltage of 500 V. The energy spectra of ²⁴¹Am and ⁵⁷Co radioisotopes were collected at room temperature and showed energy resolutions (full width at half maximum) of 2.9 and 3.6 keV for gamma rays of 59.5 and 122 keV, respectively.

1. Introduction

CdTe is an attractive compound semiconductor material for gamma-ray detectors because of its high density (5.8 g/cm³), high atomic number ($Z_{\text{Cd}} = 48$, $Z_{\text{Te}} = 52$), and high resistivity (10⁹ Ω·cm). Detectors based on CdTe can operate at room temperature because of its wide bandgap ($E_g = 1.46$ eV). CdTe detectors are preferably fabricated as diodes with a high potential barrier to reduce dark current because ohmic CdTe detectors suffer from enhanced dark current at higher biases and cannot efficiently operate at applied voltages greater than 100 V.⁽¹⁾ Diode-type detectors can operate at larger reverse bias voltages and exhibit greater charge collection efficiency and energy resolution than ohmic-type detectors.⁽²⁾ Schottky diodes are widely used for gamma-ray detectors to obtain a high energy resolution because of the low leakage current at a reverse bias and the relatively easy fabrication process.^(3,4) The Schottky barrier for a metal on a CdTe crystal, however, is strongly affected by the surface condition of the CdTe crystal and the quality of the deposition of the defined metal.⁽⁵⁾ Therefore, Schottky barriers are easily deteriorated in detector manufacturing steps such as tiling, stacking, solder bumping, and wire

*Corresponding author: e-mail: miyake.taku@anseen.com
<https://doi.org/10.18494/SAM4665>

bonding. In addition, polarization occurs in Schottky detectors.^(6,7) Therefore, a built-in p–n junction formed inside the semiconductor at a certain depth is expected to be more tolerant to external effects and to have stable characteristics desirable for practical applications.

Hatanaka *et al.* fabricated CdTe gamma-ray detectors with a built-in p–n junction.⁽⁸⁾ They used a laser-induced doping technique with a KrF excimer laser having a wavelength of 248 nm and a pulse width of 20 ns. An In film (300–400 nm) was evaporated onto the B face (Te face) of (111) CdTe crystals, and a KrF excimer laser was used to irradiate the In film. An n-type CdTe layer was formed by In diffusion into the p-like CdTe crystal. However, the KrF excimer laser induced the evaporation of the In film.⁽⁹⁾ Therefore, the optimal laser energy and repetition number of laser pulses vary from one process to another, and the optimal conditions are not stable. Therefore, we used back-side laser irradiation, where a Nd:YAG laser with a wavelength of 1064 nm and a pulse width of 8 ns was used to irradiate the CdTe side.⁽¹⁰⁾ Because CdTe is transparent to radiation with a wavelength of 1064 nm, the laser can irradiate the In–CdTe interface through the CdTe crystal.

Nishizawa *et al.* fabricated In/CdTe/Au diodes using laser-induced back-side doping with a Nd:YAG laser and subsequently evaluated their rectification characteristics.⁽¹⁰⁾ They also investigated the thermal durability of the In/CdTe/Au diodes at temperatures as high as 300 °C. They found that the current–voltage (I – V) characteristics were approximately the same before and after the diodes were heated at 300 °C. In addition, the spectral characteristics of the diodes, which were evaluated by using the diodes to collect the 60 keV gamma-ray spectrum from an ²⁴¹Am sample, exhibited approximately the same detection efficiency and energy resolution before and after the diodes were heated at 300 °C. However, they did not obtain direct evidence indicating that the laser-induced back-side doping led to n-type layer formation⁽¹⁰⁾ nor did they carry out Hall effect measurements for the In-doped area.

In the present study, we measured the Hall effect for an In-doped CdTe layer formed by laser-induced back-side doping with a Nd:YAG laser to obtain the direct evidence of the formation of an n-type layer. We then measured the I – V characteristics and evaluated the gamma-ray spectral characteristics of In/CdTe/Au p–n diodes fabricated by laser-induced back-side doping with a Nd:YAG laser.

2. Materials and Methods

We used (111)-oriented, high-resistivity, Cl-compensated p-type single-crystal CdTe wafers produced by Acrorad using the traveling heater method. The purpose of the Hall effect measurements was to obtain the direct evidence of (and determine the optimal laser energy for) the formation of an n-type layer by laser-induced back-side doping with a Nd:YAG laser. The dimensions of the samples prepared for the Hall effect measurements were $10 \times 10 \times 0.75$ mm³. The laser-induced back-side doping with a Nd:YAG laser was performed as follows. An In film with a thickness of 50 nm was deposited onto the Te face of CdTe by vacuum evaporation after CdTe substrates were cleaned with Br:MeOH solution for 90 s. A schematic of the optical setup for the back-side laser irradiation of the In/CdTe interface is shown in Fig. 1. We used a Nd:YAG laser (TRLi G 850-10, Litron Lasers) with a wavelength of 1064 nm, a repetition rate of 10 Hz,

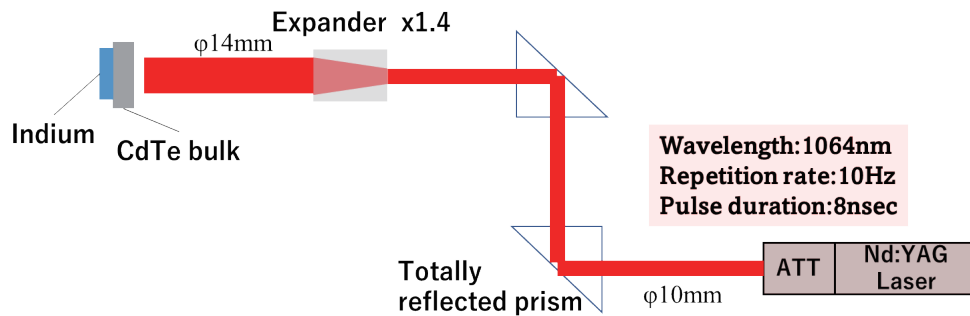


Fig. 1. (Color online) Schematic of optical setup for back-side laser irradiation of the In/CdTe interface. The laser diameter was increased from 10 to 14 mm using an expander, then the laser was irradiated through the CdTe bulk.

and a pulse width of 8 ns. The laser diameter was increased from 10 to 14 mm using an expander (ZBE11 0.5–2.5× UVFS Zoom Beam Expander, 980–1130 nm V coating, Thorlabs), then the CdTe side was irradiated with the laser. We used four energy densities—25, 50, 75, and 100 mJ/cm^2 —where the energy density was controlled by an attenuator. The repetition number of laser pulses was 50 shots. After laser irradiation, the remaining In layer was removed using HCl solution. In electrodes were then deposited onto the four corners of the laser-induced In-doped area for measurement using the van der Pauw method, and the electron concentration, resistivity, electron mobility, and Hall coefficient of each sample were measured using a Hall measurement system (HMS-500, ECOPIA). We repeated the Hall effect measurements five times and confirmed that the measured values were approximately the same; we then calculated the average values.

To fabricate the gamma-ray detectors using the In/CdTe/Au p–n diodes, we used $5 \times 5 \times 0.75$ mm^3 CdTe substrates. A guard-ring structure formed by photolithography was used to reduce the leakage current.⁽¹¹⁾ Because electrons have a higher mobility and longer lifetime than holes in CdTe, electron-collecting-type detectors, in which the anode side should be pixelated, are desirable for high energy resolution.⁽¹²⁾ Therefore, we fabricated a guard-ring structure on the anode using the lift-off process of In, although the implementation of the guard-ring structure on the anode side of In/CdTe was more difficult than that on the cathode side of CdTe/Au.⁽¹¹⁾ As shown in Fig. 2, the anode electrode was separated into two parts: a central electrode, which is the active area for gamma-ray detection, and a surrounding guard-ring electrode. The sizes of the central electrode and gap were 2.5×2.5 mm^2 and 50 μm , respectively. The laser beam was used to irradiate the In/CdTe interface through the CdTe bulk after the guard-ring structure of the In side was formed by photolithography. The laser irradiation method was the same as that used in the Hall effect measurements. We used a laser energy of 75 mJ/cm^2 because the Hall measurement showed that it was the optimal laser energy. After the n-type layer was formed, a Au electrode was deposited as a common cathode. The detector was diced to 4.6×4.6 mm^2 using an automatic dicing saw (DAD321, DISCO). Finally, the detectors were passivated with 15 wt% KOH solution. The CdTe p–n diode-type detectors were set in a test fixture (N1259A, KEYSIGHT), and the I – V characteristics were measured with a power device analyzer (B1505A, KEYSIGHT). The same bias voltage was applied to the In central and guard-ring electrodes, and

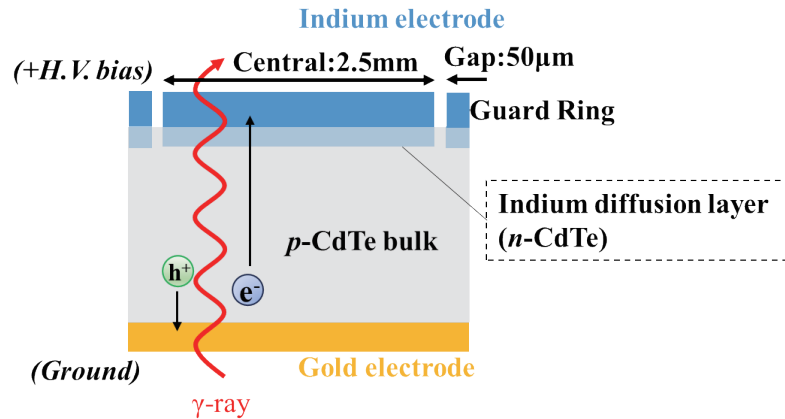


Fig. 2. (Color online) Structure of In/CdTe/Au p-n diode. The In anode electrode was separated into two parts: a central electrode, which is an active area for gamma-ray detection, and a surrounding guard-ring electrode. The same bias voltage was applied to the In central and guard-ring electrodes. We irradiated the laser beam on the In/CdTe interface through the CdTe bulk. Gamma rays were irradiated on the CdTe/Au side.

the Au bottom electrode was grounded. In spectral measurements, ^{241}Am and ^{57}Co radioisotopes were used as gamma sources to irradiate the CdTe/Au side. The CdTe detector was placed 20 mm from the gamma sources. A bias voltage of 300 V was applied to both the central and guard-ring electrodes, and the Au bottom electrode was grounded. The central electrode was connected to a charge amplifier (5102, CLEAR PULSE). The electrical pulses were fed through the main amplifier (4419HI, CLEAR PULSE) into a multichannel analyzer (MCA7700, SEIKO EG&G). The shaping time constant was 2 μs . The measurement time was 1 min. The Hall effect, I - V , and gamma-ray spectral measurements were conducted at room temperature.

3. Results and Discussion

The sign of the Hall effect indicates that all the laser-induced In-doped areas are of the n-type. We obtained the direct evidence of the formation of an n-type layer by laser-induced back-side doping with a Nd:YAG laser. Table 1 shows the dependence of the electron concentration, resistivity, and electron mobility for the laser-induced In-doped area on the laser energy density of the Nd:YAG laser. Negative carrier concentration values indicate that the carriers were electrons.

When the laser energy density was increased to 50 mJ/cm^2 , the resistivity markedly decreased and the carrier concentration and electron mobility markedly increased. As the laser energy density was further increased, the resistivity decreased and the carrier concentration and electron mobility increased. However, the carrier concentration decreased and the resistivity increased at a laser energy density of 100 mJ/cm^2 , although the electron mobility slightly increased. Therefore, we selected 75 mJ/cm^2 as the optimal laser energy density, for which the electron concentration, resistivity, and electron mobility were $2.0 \times 10^{17} \text{ cm}^{-3}$, 0.17 $\Omega\cdot\text{cm}$, and 190 $\text{cm}^2/(\text{V}\cdot\text{s})$, respectively.

Figure 3 shows the I - V characteristics of the gamma-ray detector fabricated using the In/CdTe/Au p-n diode shown in Fig. 2. The red solid and red dashed lines show the reverse leakage

Table 1

Dependence of electron concentration, resistivity, and electron mobility for the laser-induced In-doped area on the irradiation energy density of a Nd:YAG laser.

Energy density (mJ/cm ²)	Electron concentration (cm ⁻³)	Resistivity ($\Omega\cdot\text{cm}$)	Electron mobility (cm ² /V·s)
25	-5.6×10^{15}	4.3×10^5	3.9×10^{-2}
50	-1.5×10^{17}	4.6×10^{-1}	9.0×10^1
75	-2.0×10^{17}	1.7×10^{-1}	1.9×10^2
100	-6.5×10^{16}	4.6×10^{-1}	2.1×10^2

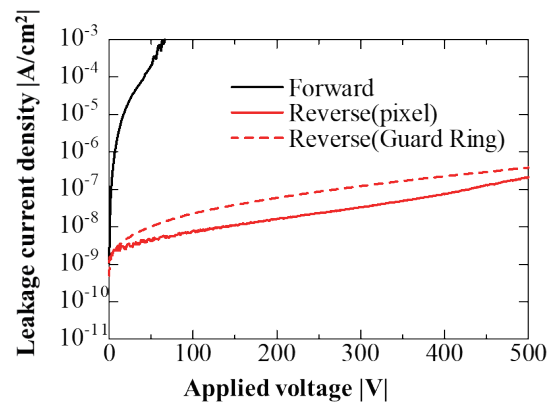


Fig. 3. (Color online) I - V characteristics of the gamma-ray detector fabricated using the In/CdTe/Au p-n diode with a guard-ring electrode on the anode side. The red solid and red dashed lines show the reverse leakage current densities of the central and guard-ring electrodes, respectively. The black solid line shows the total forward leakage current density.

current densities of the central and guard-ring electrodes, respectively. The black solid line shows the total forward current density. As illustrated in Fig. 3, rectification behavior is clearly observed, indicating that the In/CdTe/Au p-n diode exhibits diode characteristics. The leakage currents of the central and guard-ring electrodes were 13 and 57 nA at a reverse voltage of 500 V, respectively. The leakage current level of the central electrode is suitable for a gamma-ray detector. We fabricated the In/CdTe/Au p-n diode that had the In electrode on the whole anode and the Au guard-ring electrode with the same size as the In guard-ring electrode shown in Fig. 2. We measured the leakage currents of the In/CdTe/Au p-n diode with the Au guard-ring electrode at the reverse bias voltage. The leakage currents of the central and guard-ring electrodes were 240 pA and 22 nA at a reverse voltage of 500 V, respectively, indicating that both the central and guard-ring electrodes had lower leakage currents. These results indicate that the space between the central and guard-ring electrodes for the In/CdTe/Au p-n diode with a guard ring on the anode electrode might be a result of laser-irradiation-induced damage.

Figures 4 and 5 show the energy spectra of ²⁴¹Am and ⁵⁷Co radioisotopes, respectively, at room temperature. The bias voltage was 300 V. These spectra show good energy resolutions (full width at half maximum; FWHM) of 2.9 and 3.6 keV for gamma rays of 59.5 and 122 keV,

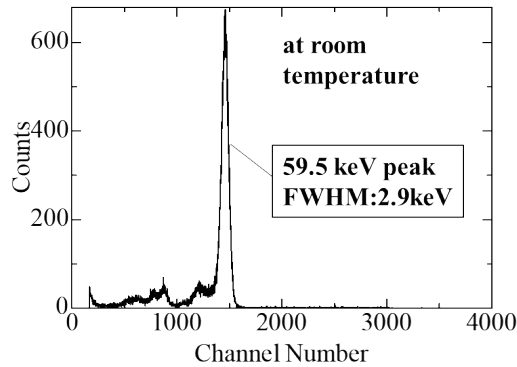


Fig. 4. Energy spectrum of ^{241}Am radioisotope for the In/CdTe/Au p-n diode with a guard-ring electrode on the anode side at room temperature. The bias voltage was 300 V.

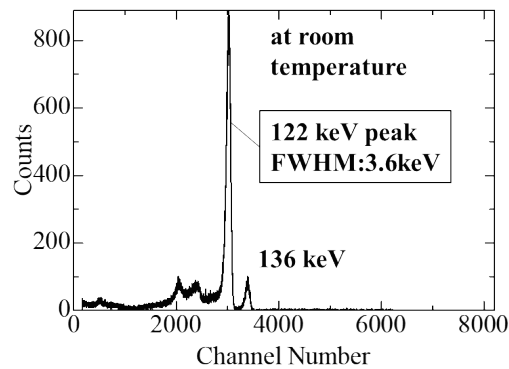


Fig. 5. Energy spectrum of ^{57}Co radioisotope for the In/CdTe/Au p-n diode with a guard-ring electrode on the anode side at room temperature. The bias voltage was 300 V.

respectively.⁽¹³⁾ Almost no tail structure is observed in the spectra. These results indicate that the In/CdTe/Au p-n diodes fabricated by laser-induced back-side doping with a Nd:YAG laser can operate as electron-collecting-type gamma-ray detectors. This is because, when the resistance of the space between the central and guard-ring electrodes decreases owing to laser-irradiation-induced damage, the area of the central electrode becomes equivalently larger, resulting in the increase in the leakage current of the central electrode.

We have measured the energy spectrum of the cathode-divided device. The cathode-divided device had energy resolutions of 3.8 and 4.3 keV for gamma rays of 59.5 and 122 keV, respectively, which are lower than those of the anode-divided device. This is because the $\mu\tau$ product of electrons is much larger than that of holes.^(14,15)

4. Conclusions

We formed an n-type layer via the laser-induced back-side doping of In metal using a Nd:YAG laser to irradiate an In/CdTe interface through the CdTe bulk. The n-type layer was confirmed by Hall effect measurements on the In-doped area. An electron concentration of $2.0 \times 10^{17} \text{ cm}^{-3}$, a resistivity of $0.17 \text{ } \Omega \cdot \text{cm}$, and an electron mobility of $190 \text{ cm}^2/(\text{V} \cdot \text{s})$ were obtained at the optimal laser energy density of 75 mJ/cm^2 . An In/CdTe/Au p–n diode with an In guard-ring electrode on the anode was fabricated as an electron-collecting-type gamma-ray detector by laser-induced back-side doping using a Nd:YAG laser. In the In/CdTe/Au p–n diode, rectification behavior was clearly observed and the leakage current of the central electrodes was 13 nA at a reverse bias voltage of 500 V. In the In/CdTe/Au p–n diode that had the In electrode on the whole anode and the Au guard-ring electrode, the leakage current of the central electrode was 240 pA at the reverse bias voltage of 500 V. These results indicate that the space between the central and guard-ring electrodes for the In/CdTe/Au p–n diode with a guard ring on the anode electrode might be the result of laser-irradiation-induced damage. The energy spectra of ^{241}Am and ^{57}Co gamma sources recorded using the In/CdTe/Au p–n diode showed good energy resolutions (FWHM) of 2.9 and 3.6 keV for gamma rays of 59.5 and 122 keV, respectively. These results indicate that the In/CdTe/Au p–n diodes with a guard ring on the In anode side, which were fabricated by laser-induced back-side doping with a Nd:YAG laser, can operate as electron-collecting-type gamma-ray detectors.

Acknowledgments

This work was supported by Acquisition, Technology & Logistics Agency (No. JPJ004596).

References

- 1 S. Del Sordo, L. Abbene, E. Caroli, A. M. Mancini, A. Zappettini, and P. Ubertini: *Sensors* **9** (2009) 3491. <https://doi.org/10.3390/s90503491>
- 2 L. A. Kosyachenko, T. Aoki, C. P. Lambropoulos, V. A. Gnatyuk, E. V. Grushko, V. M. Sklyarchuk, O. L. Maslyanchuk, O. F. Sklyarchuk, and A. Koike: *IEEE Trans. Nucl. Sci.* **60** (2013) 2845. <https://doi.org/2013.2260356>
- 3 C. Matsumoto, T. Takahashi, K. Takizawa, R. Ohno, T. Ozaki, and K. Mori: *IEEE Trans. Nucl. Sci.* **45** (1998) 428. <https://doi.org/10.1109/23.682421>
- 4 T. Takahashi, B. Paul, K. Hirose, C. Matsumoto, R. Ohno, T. Ozaki, K. Mori, and Y. Tomita: *Nucl. Instrum. Methods Phys. Res., Sect. A* **436** (2000) 111. [https://doi.org/10.1016/S0168-9002\(99\)00606-3](https://doi.org/10.1016/S0168-9002(99)00606-3)
- 5 S. M. Sze and K. K. Ng: *Physics of Semiconductor Devices* (Wiley, New Jersey, 2007) 3rd ed., Chaps.2–3, pp. 79–196. <https://doi.org/10.1002/0470068329>
- 6 H. Nakagawa, T. Terao, T. Masuzawa, T. Ito, A. Koike, H. Morii, and T. Aoki: *Sens. Mater.* **30** (2018) 7. <https://doi.org/10.18494/SAM.2018.1929>
- 7 K. Okada, Y. Sakurai, and Suematsu, *Appl. Phys. Lett.* **90** (2007) 063504. <https://doi.org/10.1063/1.2457971>
- 8 Y. Hatanaka, M. Niraula, A. Nakamura, and T. Aoki: *Appl. Surf. Sci.* **175–176** (2001) 15. [https://doi.org/10.1016/S0169-4332\(01\)00117-9](https://doi.org/10.1016/S0169-4332(01)00117-9)
- 9 V. A. Gnatyuka, T. Aoki, and Y. Hatanaka: *IEEE Trans. Nucl. Sci.* **51** (2004) 2466. <https://doi.org/10.1109/TNS.2004.836068>
- 10 J. Nishizawa, V. Gnatyuk, K. Zelenska, and T. Aoki: *Sens. Mater.* **32** (2020) 11. <https://doi.org/10.18494/SAM.2020.3054>

- 11 K. Nakazawa, K. Oonuki, T. Tanaka, Y. Kobayashi, K. Tamura, T. Mitani, G. Sato, S. Watanabe, T. Takahashi, R. Ohno, A. Kitajima, Y. Kuroda, and M. Onishi: IEEE Trans. Nucl. Sci. **51** (2004) 1881. <https://doi.org/10.1109/TNS.2004.832684>
- 12 S. Watanabe, S. Ishikawa, S. Takeda, H. Odaka, T. Tanaka, T. Takahashi, K. Nakazawa, M. Yamazato, A. Higa, and S. Kaneku: Jpn. J. Appl. Phys. **46** (2007) 6043. <https://doi.org/10.1143/JJAP.46.6043>
- 13 K. Nakazawa, T. Takahashi, S. Watanabe, G. Sato, M. Kouda, Y. Okada, T. Mitani, Y. Kobayashi, Y. Kuroda, M. Onishi, R. Ohno, and H. Kitajima: Nucl. Instrum. Methods Phys. Res., Sect. A, **512** (2003) 412. [https://doi.org/10.1016/S0168-9002\(03\)01920-X](https://doi.org/10.1016/S0168-9002(03)01920-X)
- 14 G. Sato, T. Takahashi, M. Sugiho, M. Koda, T. Mitani, K. Nakazawa, Y. Okada, and S. Watanabe: IEEE Trans. Nucl. Sci. **49** (2001) 1258. <https://doi.org/10.1109/TNS.2002.1039648>
- 15 R. Gul, J. S. McCloy, M. Murugesan, B. Montag, and J. Singh: Crystals **12** (2022) 1365. <https://doi.org/10.3390/cryst12101365>

About the Authors



Taku Miyake received his M.S. and Ph.D. degrees from Shizuoka University, Japan, in 2019 and 2022, respectively. Since 2022, he has worked for ANSeeN Inc. His research interests are in CdTe/CZT-based detectors, laser-induced doping, synthesizing diamond thin films by chemical vapor deposition, and characterizing p–n junction diodes, neutron detectors, and imaging devices. (miyake.taku@anseen.com)



Junichi Nishizawa received his B.S. and M.S. degrees from Shizuoka University, Japan, in 2015 and 2017, respectively. Since 2017, he has been a postgraduate student at Graduate School of Science and Technology, Shizuoka University. His research interests are in CdTe-based and scintillator high-energy detectors, laser-induced doping, and the formation and characterization of Schottky and p–n junction diodes, X/γ-ray pixel sensors, and imaging devices. (nishizawa@anseen.com)



Akifumi Koike received his B.S., M.S., and Ph.D. degrees from Shizuoka University, Japan, in 2007, 2009, and 2013, respectively. From 2008 to 2012, he was a scientific researcher at Shizuoka University, Japan. Since 2011, he has been on the Board of Directors at ANSeeN Inc. His research interests are in X-ray, gamma-ray, and neutron-ray detectors, and image sensors. (koike@anseen.com)



Toru Aoki received his B.Eng., M.Eng., and Ph.D. degrees from Shizuoka University, Japan, in 1991, 1993, and 1996, respectively. From 1996, he was an assistant professor then an associate professor at the Research Institute of Electronics, Shizuoka University. Since 2015, he has been a professor at Shizuoka University. He has also been the chief technology officer at ANSeeN Inc. since 2011. He is a special advisor to the president of Shizuoka University. His research interests are in material engineering, semiconductor devices, X-ray and γ-ray detectors, and CT. (aoki.toru@shizuoka.ac.jp)



Hidenori Mimura received his B.S., M.S. and Ph.D. degrees from Shizuoka University, Japan, in 1979, 1981, and 1987, respectively. From 1987 to 1994, he was a senior researcher at Nippon Steel Corporation, Japan. From 1994 to 1996, he was a senior researcher at Advanced Telecommunication Research Institute (ATR), Japan. From 1996 to 2003, he was an associate professor at Tohoku University, Japan. Since 2003, he has been a professor at Shizuoka University. His research interests are in radiation sensors. (mimura.hidenori@shizuoka.ac.jp)

